



Genetic Expression Programming Based Empirical Models for the Prediction of Rutting Parameter of Bitumen Modified Using Nanomaterials

Sandra Matarneh,^{1,*} Nawal Louzi,¹ Ibrahim Asi,¹ Mu'tasim Abdel-Jaber² and Eyad Masad^{3,4}

Abstract

Bitumen rheological properties significantly influence pavement performance in terms of resistance to rutting and cracking. Various approaches, such as polymer modification and the incorporation of nanomaterials, have been employed to improve bitumen properties. This study aims to characterize bitumen modified with different concentrations of nano-hydrated lime (NHL), nano-clay (NC), and nano-olive husk (NOH). The rutting parameter ($G^*/\text{Sin}\delta$) of these materials was evaluated using the dynamic shear rheometer (DSR) under unaged and short-term aged conditions at various temperatures. Consequently, a robust experimental dataset was employed to develop prediction models for each nanomodified bitumen using genetic expression programming (GEP). The models incorporated various variables: temperature, loading frequency, rutting parameter of the unmodified bitumen, and the concentration of nanomaterials. The findings demonstrated that GEP provided precise and insightful expressions for estimating the $G^*/\text{Sin}\delta$ of nanomodified bitumen. The results demonstrated that incorporating 10% NC significantly enhanced rutting resistance. While using 5% NOH improved the bitumen property, its effectiveness diminished at a higher concentration of 10% due to potential issues like agglomeration and NOH's oil content. Using 5% NHL was the most viable option when considering performance alongside cost-effectiveness. Evaluating cost, compatibility with bitumen, and environmental impact is crucial when considering various nanomaterials as binder modifiers.

Keywords: Viscoelastic properties; Rutting parameter; Gene-expression programming; Genetic expression programming; Nanomodified asphalt.

Received: 04 February 2025; Revised: 20 February 2025; Accepted: 05 March 2025.

Article type: Research article.

1. Introduction

Bitumen, derived from crude oil and oil sand, is a heavy hydrocarbon mixture with high resin-asphaltene content, characterized by its high viscosity and density is extensively utilized in pavement construction.^[1,2] It is characterized and graded based on its rheological properties related to resistance to rutting, fatigue cracking, and low-temperature cracking. Bitumen must maintain adequate stiffness and elasticity at

elevated service temperatures, while it should exhibit relatively low stiffness and maintain elasticity at low and medium temperatures to prevent cracking.^[3] The use of geosynthetics in flexible pavements not only enhances their structural performance and longevity but also contributes to environmental sustainability and cost reductions, making them a viable option for modern road construction.^[4,5] Moreover, to function effectively, bitumen must exhibit sufficient fluidity at high mixing temperatures (approximately 160 °C) to coat aggregates thoroughly. With the increasing demands posed by rising traffic loads and severe weather conditions driven by global climate change, unmodified bitumen may not meet the required performance standards. Consequently, modifying bitumen is critical to improving its resistance to heavy traffic loads and temperature fluctuations.^[6,7]

The application of nanomaterials in bitumen modification

¹ Civil Engineering Department, Faculty of Engineering, Al-Ahliyya Amman University, Amman, 19111, Jordan

² Department of Civil Engineering, Faculty of Engineering, The University of Jordan, Amman, 11942, Jordan

³ College of Science and Engineering, Hamad Bin Khalifa University, Qatar Foundation, Doha, P.O. Box 34110, Qatar

⁴ Mechanical Engineering Program, Texas A&M University at Qatar, Doha, P. O. Box 23874, Qatar

*Email: s.matarneh@ammanu.edu.jo (S. Matarneh)

has demonstrated the potential to enhance bitumen properties and pavement performance. For example, Qadir *et al.*^[8] highlighted the effects of nano-clay (NC) on bitumen properties while exploring the incorporation of NC and styrene-butadiene-styrene (SBS) into asphalt mixtures. Mousavinezhad *et al.*^[9] indicated significant improvements in rheological properties and enhanced rutting resistance. Similar studies by Ghanoun *et al.*^[10] and Zahid *et al.*^[11] confirmed the positive effects of NC on bitumen performance.

Nano-hydrated lime (NHL) has also been widely studied for its impact on bituminous materials. Alfaqawi *et al.*^[12] conducted a study on the effect of NHL fillers on the rheological properties and cracking behavior of mastics. This study demonstrated that NHL substantially enhanced the rutting resistance of mastics and decreased their aging susceptibility. Similarly, Rasouli *et al.*^[13] performed an analogous study assessing the impact of laboratory aging on the fatigue behavior of mixtures using NHL.^[14] The experimental results indicated that 1%, 1.5%, and 2% of NHL improved the fatigue life of bituminous mixtures. Several other studies further verified the effectiveness of the NHL in improving performance.^[15]

Nano-olive husk (NOH) has also been evaluated as another promising bitumen nano modifier. Research shows that NOH reduced penetration and ductility while increasing the softening point of bitumen.^[16] NOH enhanced the stability and reduced the flowability of mixtures, particularly at concentrations of 10-15% of bitumen mass.^[17] Another study indicated that NOH improved creep stiffness by as much as 15% by augmenting the adhesive bond between bitumen and aggregate.^[18] The influence of prina produced by olive oil processing on the rheological and physical properties of bitumen was investigated.^[19] Samples modified using NOH exhibited a reduction in penetration and ductility and an increase in the softening point, attributed to the higher viscosity of the NOH bitumen. The penetration index of the modified samples demonstrated a 58% reduction in temperature sensitivity. Physical and rheological evaluations identified 15% as the optimal proportion of prina in bitumen, significantly enhancing rutting resistance at elevated temperatures and improving resistance to thermal cracking.^[19] Aitkaliyeva *et al.*^[20] highlighted a promising pathway for using oil sludge not just to restore aged asphalt but also to foster more sustainable practices in road maintenance while addressing significant waste disposal issues.

It is beneficial to express and predict the properties of nanomodified binders using mathematical models. For this purpose, empirical modeling of material properties is often achieved with regression models and the genetic expression

programming (GEP) approach. GEP is an advanced algorithm that enhances traditional genetic programming (GP) by introducing a distinct genotype-phenotype mapping mechanism.^[21] A significant advantage of GEP over traditional regression models is the ability to capture complex, nonlinear relationships inherent in material properties. Moreover, studies have shown that GEP often achieves higher predictive accuracy than traditional regression models.^[22]

This study investigates the effects of NH, NC, and NOH on bitumen performance in terms of changes in the rutting parameter ($G^*/\text{Sin}\delta$) for both unaged and short-term aged samples. Four nanomaterial concentrations by bitumen weight (1%, 3%, 5%, and 10%) were used in this study. Consequently, mathematical GEP-based models were created to predict the $G^*/\text{Sin}\delta$ of unmodified and modified bitumen incorporating NHL, NC, and NOH.

2. Materials and methods

The research was conducted in two stages. In the first stage, a comprehensive laboratory study was performed to assess the impact of nanomaterial concentration on bitumen rutting resistance. In the second stage, a prediction model was developed using GEP. The methodology employed to conduct this investigation is outlined as follows.

2.1 Bitumen

This study utilized a bitumen with a penetration grade of AC-60/70 supplied by Jordan Petroleum Refinery Company (JPRC) in Jordan. The high-temperature performance grade of this bitumen is PG 58. Table 1 presents the basic properties of the AC-60/70 bitumen.

Table 1: The physical properties of the used AC-60/70 bitumen.

Properties	Values	Standard
Penetration 0.1 mm at 25 °C	63.4	ASTM D5
Softening point (°C)	58	ASTM D36
Ductility at 25 °C (in cm)	+100	ASTM D113
Rotational viscosity at 135 °C (CP)	561.3	ASTM D4402

2.2 Nanomaterial modifiers

Nano-hydrated lime is synthesized by processing conventional hydrated lime (calcium hydroxide, $\text{Ca}(\text{OH})_2$) into nanoparticles. The nanometer-scale dimensions significantly enhance its surface area and reactivity relative to conventional hydrated lime. Nano clay denotes tiny particles of naturally occurring clay minerals, such as montmorillonite, kaolinite, or bentonite, that have been treated to the nanometer scale. The nano-clay particles possess a stratified structure, and their elevated aspect ratio renders them very efficient as reinforcements in diverse materials. Nano olive husk is a

nanomaterial obtained from the agricultural residue of olive processing, particularly the husks or pits remaining after olive oil extraction. The husks are reduced to nano-scale particles using various operations, including grinding and high-energy milling. These particles have distinctive physical and chemical characteristics, including a substantial surface area, increased reactivity, and possible pozzolanic activity, making them appropriate for bitumen modification.

Dynamic light scattering (DLS) is a method whereby a monochromatic laser beam is passed through a biomolecular solution, and the variations in scattered light intensity are examined. The procedure is noninvasive, requires just 12 μL of material, and may swiftly provide information about the size and uniformity of biomolecules within minutes. Sample features such as aggregation, folding, or conformation may be seen in relation to different preparations, solvent conditions, temperature, or duration. DLS measurement, peaks corresponding to NHL, NC, and NOH were detected in the charge transfer spectra. This study used a laser diffraction method that integrates various scattering methods to determine the particle size distribution of nanoparticles. The results indicate that the nanoparticles referenced exhibit a particle size distribution, as shown in Table 2.

Table 2: Particle size for modifiers NHL, NC, and NOH.

Modifier	Average particle size (nm)
Nano hydrated lime (NHL)	154.2
Nano clay (NC)	190.1
Nano olive husk (NOH)	104.9

2.3 Sample preparation

Modifications were conducted relative to the weight of the original bitumen. Four concentration percentages of each nanomaterial were applied, resulting in one unmodified sample and twelve nanomodified samples, as shown in Table 3. The blending process was carefully standardized using a mechanical mixer operated at 120 rpm for 120 minutes at a temperature of 160 °C. The study indicates that a heating temperature of 150 °C for a length of 2 hours is an appropriate strategy for proper preparation prior to normal laboratory testing, with no impact on ageing during sample preparation.^[23] Standardized conditions included the type of mixer (mechanical) used to achieve a homogeneous blend, the mixer's rotational speed, the blending duration, and the temperature maintained throughout the process.

2.4 Sample testing

The dynamic shear rheometer (DSR) from Bohlin Instruments DSR II10 INT was used to measure the dynamic modulus (G^*)

and phase angle (δ). The dynamic modulus (G^*) represents the total resistance of the material to shear deformation, encompassing both elastic and viscous components, while the phase angle (δ) reflects the relative contributions of elastic and viscous behavior. The DSR test was conducted at a frequency of 10 rad/s following ASTM D7175.^[24] The test was conducted at a strain level of 10%, ensuring it remained within the linear viscoelastic range. According to DSR criteria for rutting resistance, the $G^*/\sin\delta$ value should exceed 1 kPa for unaged asphalt binders and 2.2 kPa for binders subjected to aging through the rolling thin-film oven (RTFO) process. Various nano-modifiers affect bitumen performance under distinct loading frequency and strain magnitudes. This document presents a comprehensive comparison of NHL, NC, and NOH on their effects under these settings. Tables 4 and 5 present the effect of frequency and strain level on modified bitumen (NHL, NC, NOH).

Table 3: Samples preparation conditions.

Nanomodifier	Code	Concentration (wt% of original bitumen)
-	Control	-
Nano hydrated lime	NHL1	1%
	NHL3	3%
	NHL5	5%
	NHL10	10%
	NC1	1%
Nano clay	NC3	3%
	NC5	5%
	NC10	10%
	NOH1	1%
Nano olive husk	NOH3	3%
	NOH5	5%
	NOH10	10%

3. Results and discussion

Figs. 1-3 present representative test results at different temperatures. As expected, the shear modulus (G^*) decreased while the phase angle (δ) increased with an increase in temperature. With rising temperature, the G^* of bitumen diminishes, but the δ escalates owing to many interconnected elements. Thermal softening diminishes intermolecular tensions, enabling bitumen molecules to move with more mobility, resulting in a reduction of stiffness. The shift from an elastic-dominant to a viscous-dominant state leads to heightened energy dissipation, hence increasing δ .^[25]

The results for various samples under two conditions, unaged (ordinary) and short-term aged (RTFO-aged), are presented in Fig. 1a and b. The findings, illustrated in Fig. 1,

Table 4: Effect of frequency on modified bitumen.

Modifier	High frequency ($\omega \uparrow$) (Fast loading, short-duration stress)	Low frequency ($\omega \downarrow$) (Slow loading, long-duration stress)
Nano-Hydrated Lime (NHL)	<ul style="list-style-type: none"> Increases <i>stiffness</i> (G)**, reducing deformation. Reduces phase angle (δ), making bitumen more elastic. Improves fatigue resistance under high-frequency traffic. Creates a layered structure that resists deformation. 	<ul style="list-style-type: none"> Reduces excessive softening by maintaining stiffness. Improves rutting resistance, especially at high temperatures. Slows bitumen oxidation and aging.
Nano-Clay (NC)	<ul style="list-style-type: none"> Improves elasticity, delaying microcrack formation. Can make bitumen slightly brittle at very high frequencies. Polyphenols and lignin increase elasticity at high frequencies. 	<ul style="list-style-type: none"> Maintains structure, reducing permanent deformation. Improves low-frequency resistance, but excessive NC content may cause brittleness.
Nano-Olive Husk (NOH)	<ul style="list-style-type: none"> Enhances fatigue resistance, reducing microcracking. Phase angle (δ) stays moderate, balancing stiffness and flexibility. 	<ul style="list-style-type: none"> Antioxidant properties reduce aging and softening. Improves long-term resistance to rutting and thermal cracking. Provides better adhesion to aggregates.

Table 5: Effect of strain level on modified bitumen.

Modifier	Low strain ($\gamma \downarrow$) – Linear viscoelastic (LVE) range	High strain ($\gamma \uparrow$) – Nonlinear viscoelastic behavior
Nano-Hydrated Lime (NHL)	<ul style="list-style-type: none"> Minimal effect in the LVE range. Provides stable rheological properties. Maintains <i>moduli</i> (G, G')* within predictable limits. 	<ul style="list-style-type: none"> Delays onset of nonlinear behavior. Reduces softening under heavy loads, preventing excessive deformation. Enhances fatigue resistance but may lead to slight stiffness increase.
Nano-Clay (NC)	<ul style="list-style-type: none"> Slight increase in viscosity, leading to higher initial stiffness. Remains stable at low strains. 	<ul style="list-style-type: none"> Strong shear-thinning resistance, reducing deformation under high stress. Excessive NC content may cause brittle failure under extreme strain.
Nano-Olive Husk (NOH)	<ul style="list-style-type: none"> Improves modulus stability, keeping bitumen flexible. Maintains an ideal balance between stiffness and elasticity. 	<ul style="list-style-type: none"> Resists softening at high strain levels. Polyphenols and lignin delay material breakdown, improving crack resistance. Prevents sudden failure, making it ideal for flexible pavements.

show that for the control bitumen in its unaged state, the $G^*/\sin\delta$ value exceeds the threshold of 1.0 kPa at all temperatures except at 64 °C. However, with the addition of NHL, the $G^*/\sin\delta$ exceeded the threshold of 1.0 kPa. The experimental outcomes also demonstrate that unaged and short-term aged bitumen experienced significant improvements in $G^*/\sin\delta$ with the incorporation of NHL at various concentrations. The optimal performance was observed at 5% NHL, highlighting its efficacy in enhancing the rutting resistance of bitumen, which is aligned with previous studies.^[26-28] Using 10% NHL may have caused particle agglomeration, leading to inconsistent dispersion

within the bitumen matrix. This generates weak areas and diminishes the material's capacity to withstand strain evenly at high temperatures, adversely affecting the rutting resistance.^[29] Fig. 2 illustrates the impact of NC on the rutting parameter in both unaged (Fig. 2a) and RTFO-aged (Fig. 2b) conditions. The incorporation of NC enhances the $G^*/\sin\delta$ parameter of the binders, thereby improving their overall performance characteristics. It has been shown that nano-clay may improve rutting resistance in unaged, with a dose of 5% being the most effective. An analysis of the rutting parameter reveals that the bitumen sample containing 10% NC performs best among the tested samples for aged.

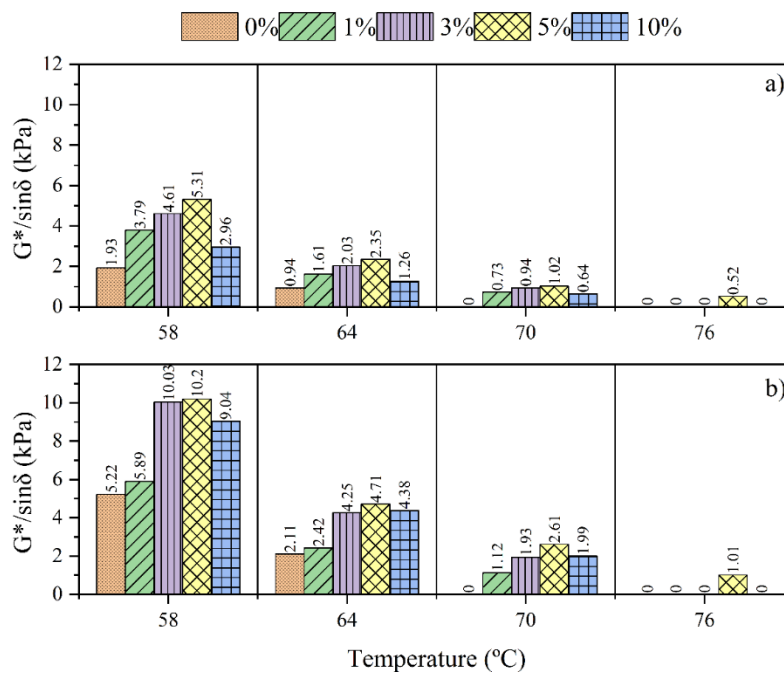


Fig. 1: The rutting parameter results for bitumen with 1%, 3%, 5%, and 10% NHL: a) Unaged and b) RTFO aged.

Fig. 3 illustrates the correlation between $G^*/\sin\delta$ and temperature for unaged samples (Fig. 3a) and RTFO-aged samples (Fig. 3b). In both unaged and short-term aged conditions, adding varying percentages of NOH increased the $G^*/\sin\delta$, with the most significant improvement observed mostly at 5% NOH. However, further increases in NOH concentration resulted in diminishing returns. The determinants influencing performance at NOH concentrations beyond 3% remain ambiguous; still, they may be associated with the composition of NOH and the quantity of oil in these combinations. As the concentration of NOH escalates, the

interaction between the NOH constituents and bitumen may become more intricate, possibly resulting in adverse consequences. The oil concentration in NOH may function as a plasticiser, diminishing the binder's rigidity and, thus, its susceptibility to rutting and persistent deformation. Moreover, elevated concentrations may lead to compatibility challenges, yielding a less uniform mixture and erratic performance. Consequently, whereas reduced quantities of NOH may enhance rheological qualities, levels beyond 3% might present complications that need more investigation and optimisation.

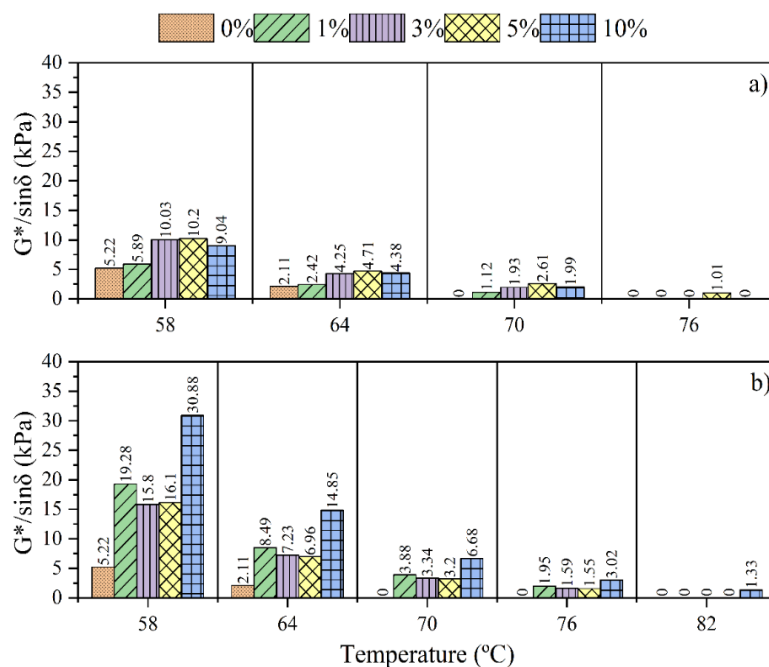


Fig. 2: The rutting parameter results for bitumen with 1%, 3%, 5%, and 10% NC: a) Unaged and b) RTFO aged.

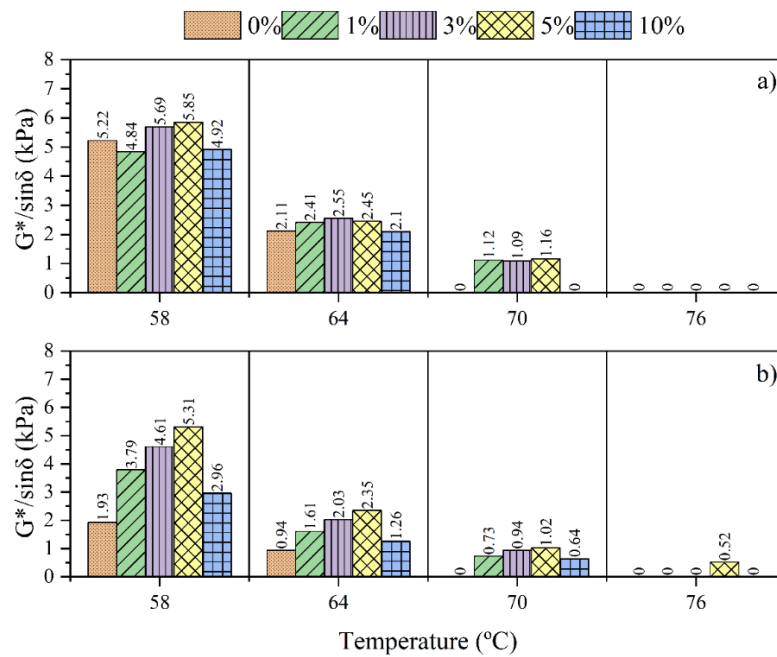


Fig. 3: The rutting parameter results for bitumen with 1%, 3%, 5%, and 10% NOH: a) Unaged and b) RTFO aged.

3.1 Gene expression programming

This study presents GEP as a computational approach to predict the rutting parameter of bitumen modified with nanomaterials. The goal is to create empirical models representing the intricate nonlinear interactions between bitumen and nanomaterials. The GEP process begins with the initial population's random generation of fixed-length chromosomes. Subsequently, each chromosome is translated into a corresponding K-expression and evaluated for its fitness. Based on fitness scores, chromosomes are selected and modified using roulette wheel sampling with elitism. This selection method ensures that the best-performing chromosomes are preserved and replicated in the next generation, maintaining the integrity of optimal solutions. The

subsequent generation undergoes the same procedure, creating new chromosomes through genetic operations such as mutation, crossover, and inversion. This iterative process continues for a predetermined number of cycles or until an optimal solution meeting the fitness criteria is achieved.^[30,31] The expression $\times, -, +, \ln, A, B, C, 5$ may be instead represented as the expression tree (ET) seen in Fig. 4, which begins at the root and sequentially traverses the string.

3.2 Model development

To establish a prediction GEP model for calculating the rutting parameter ($G^*/\sin\delta$) of modified binders at 64°C in both unaged and aged conditions, it is crucial to incorporate all relevant GEP configuration parameters derived from the

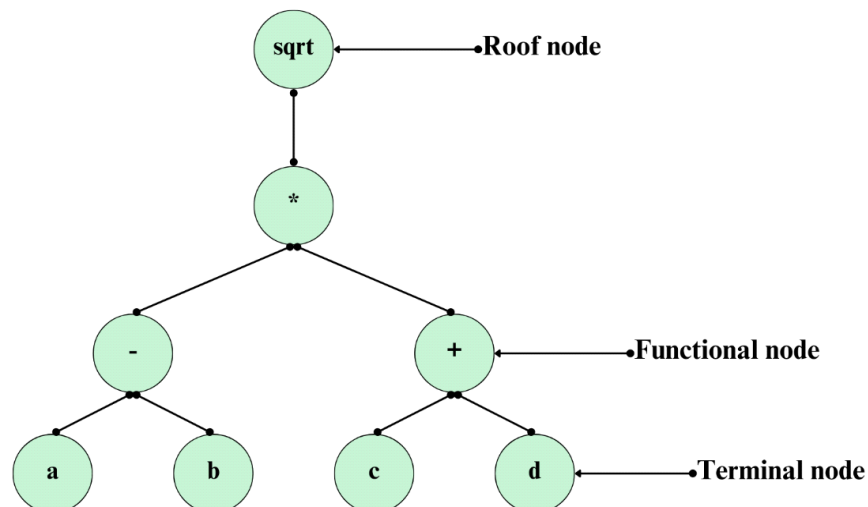


Fig. 4: Expression tree representation.

experimental program, the configuration parameters in Table 6 are essential in determining the performance and complexity of GEP models. The function set, head size, and genetic factors delineate the model's adaptability and intricacy, affecting its capacity to discern complicated correlations among data. The population size (chromosomes) and the rates of recombination, mutation, and inversion influence the equilibrium between exploration and exploitation, hence affecting the algorithm's efficacy in identifying optimum solutions. Increased mutation and recombination rates promote exploration, enhancing variety while perhaps hindering convergence. Conversely, reduced rates may facilitate expedited convergence but pose the danger of premature optimisation. The fixed parameters per gene and the linking function influence gene interactions and their contributions to the solution, while gene recombination and transportation rates affect variety and resilience. Fine-tuning these parameters is crucial for balancing model complexity, interpretability, and computing efficiency, hence assuring optimum performance of the GEP model for the specified job.

The concentration of the modifier added to modify the original bitumen significantly impacts the viscoelastic behavior of the modified bitumen. As a result, the rutting parameter ($G^*/\sin\delta$) at 64°C, representing a key viscoelastic parameter, was modeled as a function of the input parameters. These relationships are described by Eqs. (1) and (2), reflecting the dependency of $G^*/\sin\delta$ on the identified variables:

$$(G^*/\sin\delta) \text{ at } 64^\circ\text{C, Unaged} = f((G^*/\sin\delta)_0, P) \quad (1)$$

$$(G^*/\sin\delta) \text{ at } 64^\circ\text{C, Aged} = f((G^*/\sin\delta)_0, P) \quad (2)$$

where $G^*/\sin\delta$ denotes the rutting parameter of the original bitumen unaged and aged, $f(G^*/\sin\delta)$ represents function of rutting parameter and 0, and P represents the percentage (%) of the additive (NHL, NC, and NOH) included in the original bitumen.

3.3 Development and formulation of GEP models

The GEP models were developed using a single input parameter, P , for each modifier, as each modifier uniquely influenced the rutting parameter behavior of the original asphalt due to its specific properties. To develop precise GEP models for each target parameter, multiple iterations were conducted, with performance assessed using metrics such as the correlation coefficient (R^2), mean absolute error (MAE), and root mean square error (RMSE). In genetic programming, the population size, representing the number of chromosomes, dictates the number of programs created during the modeling

process. The population size determines the duration of the procedure. A population size of 40 was used in this research for GEP modelling. The head size governs the model's structure created by the software, which in turn delineates the complexity of each term, while the head size dictates the quantity of sub-ETs. In this investigation, head size and genes were assigned values of 9 and 2, respectively.

Table 6: GEP configuration parameter.

Sample code	Type of mixer
Function set	+, -, *, /, x^2
Genes	2
Chromosomes	40
Head Size	9
Linking Function	Addition
Constant per gene	3
Mutation rate	0.05
Inversion rate	0.1
Transposition rate	0.1
One-point recombination rate	0.25
Two-point recombination rate	0.25
Gene recombination rate	0.1
Gene transportation rate	0.1

The number of genes per chromosome and the head size, which are critical architectural features of GEP, significantly influence the structure of each term within the model. The number of genes determines the total number of terms, while the head size dictates the complexity of each term. For this study, two genes (ET1 and ET2) and a head size of 9 were selected. An additional linking function was applied to integrate the mathematical terms encoded by multiple genes. Three parameter sets, two genetic factors, and one head size, which produced 20 distinct parameter combinations. Each combination was replicated 10 times, resulting in 2574 GEP runs. Fundamental arithmetic operators and commonly used mathematical functions were employed to construct the GEP models for each target parameter. Among the generated models, those with the highest R^2 values and lowest RMSE scores were identified as optimal. From the 10 statistically robust models developed for each target parameter, one was selected based on the theoretical principles outlined in the experimental design. The GEP algorithm was executed using GeneXproTools.

The optimal GEP models were chosen according to the predefined selection criteria. A noteworthy observation is that the division operator appeared consistently in all the leading models for $G^*/\sin\delta$ prediction across all three additives. This recurring feature, observed over multiple generations of GEP

training, may be attributed to the division operator's suitability in accurately capturing the relationships and interactions influencing the $G^*/\sin\delta$ values of modified asphalt. This result underscores the importance of the operator's role in the predictive modeling process.

3.3.1 GEP formulation and ET for NHL-modified bitumen Eqs. (3) and (4), derived from these sub-trees, serve as mathematical models that describe the behavior of the rutting parameter ($G^*/\sin\delta$) as a function of the proportion of NHL incorporated into the asphalt. These equations provide significant insights into the rutting parameter based on different concentrations of NHL.

$$\left(\frac{G^*}{\sin\delta}\right)_{NHL\%Unaged} = \frac{-9.593 + (-5.384 + NHL)^2}{-9.229} + \frac{NHL}{5.492 * NHL - 4.051} + 4.051 \tag{3}$$

$$\left(\frac{G^*}{\sin\delta}\right)_{NHL\%Aged} = \frac{-6.735}{(1.81 * NHL + 1.638) - (1.81 * NHL^2)} + 9.973 \tag{4}$$

3.3.2 GEP formulation and ET for NC-modified bitumen

This approach emphasizes GEP's capacity to provide clear, interpretable equations that accurately reflect the experimental behavior of NC-modified bitumen, serving as a dependable and resilient tool for performance prediction. Eqs. (5) and (6) serve as mathematical models that characterize the behavior of the rutting parameter ($G^*/\sin\delta$) in relation to the proportion of NC included in a bitumen.

$$\left(\frac{G^*}{\sin\delta}\right)_{NC\%Unaged} = 2 + \frac{NC}{(6.514 + 3.257 * NC) - (NC^2)} + \frac{NC}{(2 * NC - 1.464) * NC} \tag{5}$$

$$\left(\frac{G^*}{\sin\delta}\right)_{NC\%Aged} = 2 * NC + \frac{NC}{(3.973 * NC - 3.32)} + 8.134 \tag{6}$$

3.3.3 GEP formulation and ET for NOH-modified bitumen

Eqs. (7) and (8) derived from these expression trees serve as mathematical models that characterize the behavior of the rutting parameter ($G^*/\sin\delta$) in response to the proportion of NOH incorporated into the bitumen.

$$\left(\frac{G^*}{\sin\delta}\right)_{NOH\%Unaged} = \frac{2 * NOH - 1.501}{2 * NOH + 0.642} - (0.283 * NOH) + 4.259 \tag{7}$$

$$\left(\frac{G^*}{\sin\delta}\right)_{NOH\%Aged} = \frac{(2 * NOH)}{50.415 - NOH^2} - \frac{-0.237 + \left(\frac{NOH}{-4}\right)}{-4 + (3 * NOH)} + 5.311 \tag{8}$$

3.4 Validity of the GEP models

In this study, it is considered that the coefficient of determination (R^2) value must exceed 0.8, and the error metrics, such as RMSE, should be minimized for a model to be deemed valid.^[32] These statistical criteria were rigorously evaluated for the training and validation datasets across all selected prediction models.

Figs. 5-7 present scatter plots illustrating a solid relationship between the experimental data and the predictions generated by the GP models, confirming their reliability. Golbraikh *et al.*^[33] were also applied to validate the proposed formulas using the verification dataset externally. According to these criteria, the slopes of the regression lines (k and k'), which pass through the origin, should be approximately 1, with acceptable ranges defined as $0.85 < k, k' < 1.15$. These validations further substantiate the precision and resilience of the models explained in Eqs. (9) and (10).

$$k = \frac{\sum_{i=1}^n E \times P}{E^2} \tag{9}$$

$$k' = \frac{\sum_{i=1}^n E \times P}{P^2} \tag{10}$$

where E represents the experimental data, and P denotes the GEP predicted values.

Fig. 5 illustrate the relationship between the predicted and experimental $G^*/\sin\delta$ values for NHL-modified bitumen binders under both unaged and aged conditions. In the unaged state (Fig. 5a), the regression line $y=0.9855x-0.0418$ achieves an R^2 value of 0.996, signifying exceptional predictive accuracy. The slope, which is close to 1, reflects a strong correlation between the predicted and experimental values, with data points aligning closely to the line of equality. In the aged condition (Fig. 5b), the regression line $y=1.0015x-0.0644$ with an R^2 value of 0.997 further validates the model's precision. The slope, nearly equal to 1, emphasizes the model's ability to predict experimental outcomes with minimal variance accurately. Both figures demonstrate a strong correlation between predictions and experimental results, underscoring the model's reliability and robustness in forecasting the rutting parameter for NHL-modified binders under various conditions. The slightly higher accuracy observed in the aged condition highlights the model's effectiveness in predicting the long-term performance of modified asphalt binders.

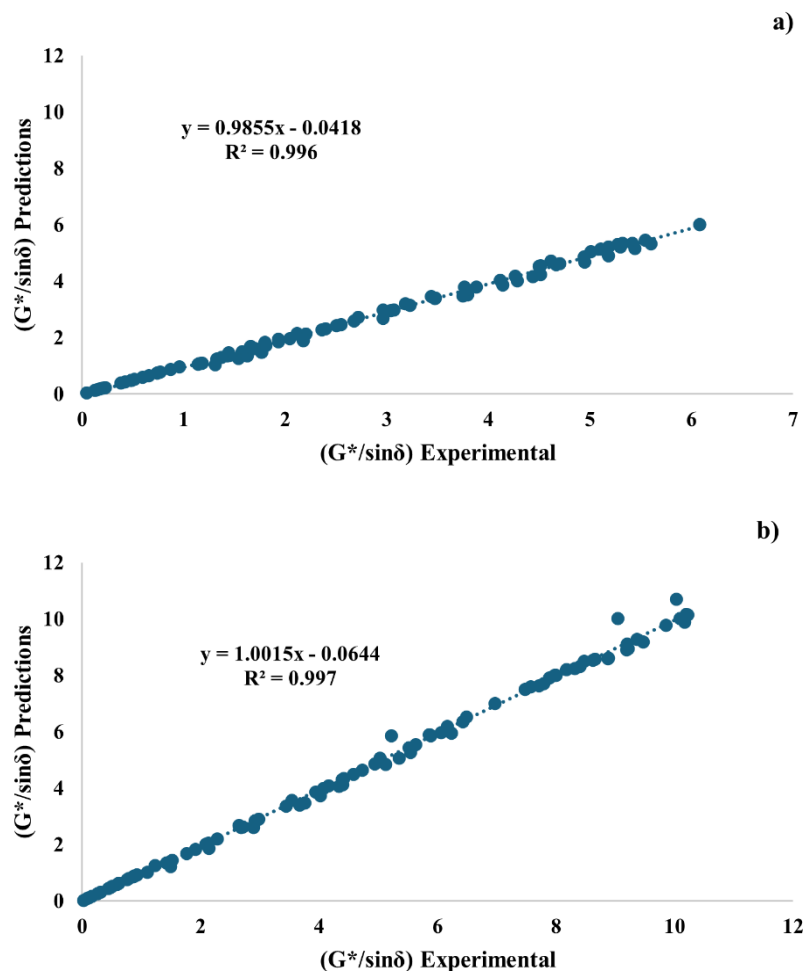


Fig. 5: Experimental versus GEP model predictions for NHL-modified bitumen: a) Unaged and b) RTFO aged.

Fig. 6 presents scatter plots illustrating a strong linear relationship between experimental results and model predictions. For the unaged samples (Fig. 6a), the trendline equation is $y=1.0059x-0.1001$, with an R^2 value of 0.997, indicating exact predictions with minimal variation. The slope, close to 1, and the intercept, near 0, confirm that the GEP model effectively captures the behavior of NC-modified bitumen in its unaged state.

For the RTFO-aged samples (Fig. 6b), the trendline equation is $y=0.9913x+0.0133$, with an R^2 value of 0.998, emphasizing the model's robustness and accuracy. While the slope slightly deviates from 1, the high R^2 value indicates excellent predictive performance even after aging. The minor underestimation observed at higher experimental values has a negligible impact on the overall reliability of the model.

The strong correlation between experimental and predicted values validates the GEP model's suitability for practical applications in evaluating and optimizing modified bituminous materials. These results highlight the model's ability to accurately assess the performance of NC-enhanced

bitumen under both unaged and aged conditions.

Fig. 7 compares the observed $G^*/\sin\delta$ values with the predictions generated by the GEP model for NOH-modified bitumen. In Fig. 7a, the unaged samples demonstrate a strong linear correlation between experimental and predicted values, as indicated by the trendline equation $y=0.9793x-0.0315$ and an R^2 value of 0.991. The slope, close to 1, confirms that the GEP model accurately predicts the behavior of unaged NOH-modified asphalt binder, with only minor underestimations observed at higher experimental values. In Fig. 7b, the trendline equation for the RTFO-aged samples is $y=0.9856x-0.0408$, with an R^2 value of 0.996, indicating even greater predictive accuracy. The slope, which is close to 1, highlights the model's ability to maintain its predictive performance post-aging, with negligible discrepancies from the experimental data. The consistently high R^2 values in both cases underscore the robustness and reliability of the GEP model in forecasting the rheological properties of NOH-modified bitumen under various aging conditions. These findings demonstrate the model's capability to accurately

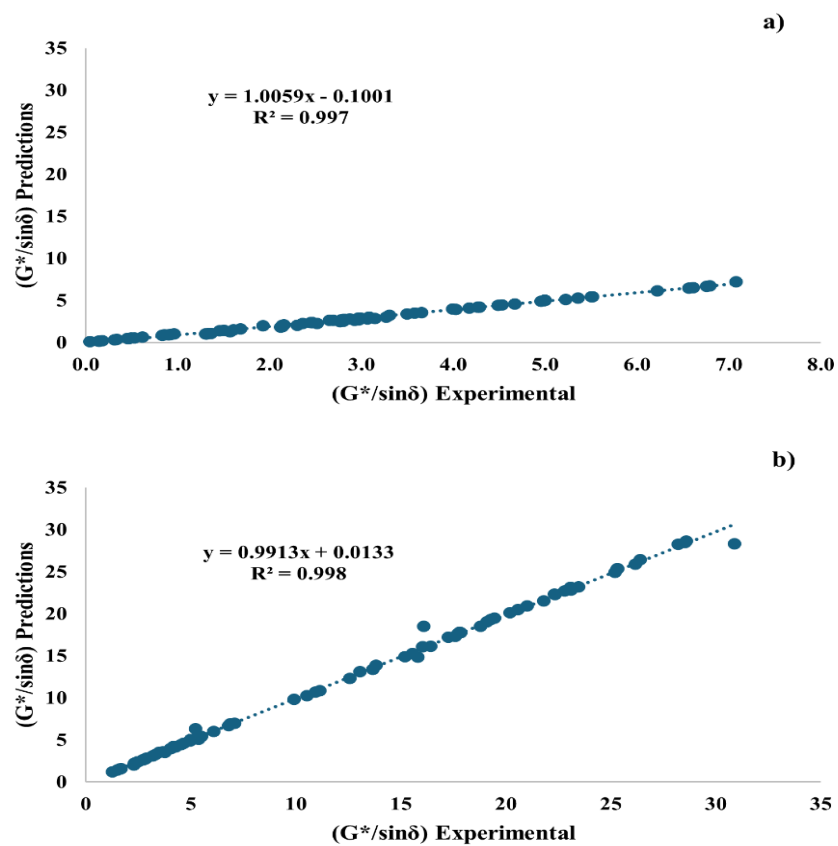


Fig. 6: Experimental versus GEP model predictions for NC- modified bitumen: a) Unaged and b) RTFO aged.

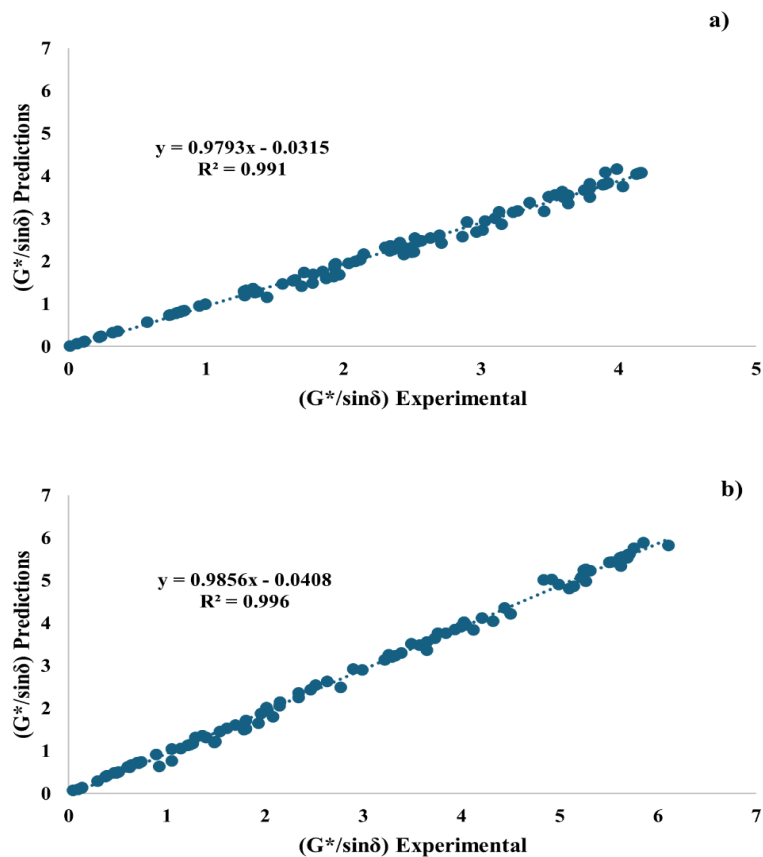


Fig. 7: Experimental versus GEP model predictions for NOH- modified bitumen: a) Unaged and b) RTFO aged.

assess the performance of modified materials, reinforcing its applicability in real-world scenarios.

Table 7 presents the validation parameters (k and k') for the rutting parameter ($G^*/\sin\delta$) of asphalt binders modified with NHL, NC, and NOH. The validation parameters are close to 1 in all cases, indicating a strong agreement between predicted and experimental results. For NHL, the validation parameters in the unaged state ($k=0.986$, $k'=0.982$) and the aged state ($k=1.002$, $k'=0.993$) demonstrate exceptional prediction accuracy, with minimal divergence post-aging. Similarly, NC exhibits high precision, with validation values of ($k=1.006$, $k'=0.997$) in the unaged condition and ($k=0.991$, $k'=0.990$) in the aged condition.

Although NOH shows slightly lower precision compared to NHL and NC, its validation parameters remain satisfactory, with ($k=0.979$, $k'=0.971$) in the unaged state and ($k=0.986$, $k'=0.981$) in the aged state. These results affirm the effectiveness of the models in predicting the rutting parameter across all modifiers, with NHL and NC exhibiting superior performance. Overall, the findings underscore the efficacy of these modifiers in enhancing rutting resistance and highlight the predictive reliability of the models, which remains consistent despite the effects of aging.

Table 7: GEP Statistical analysis for the training and validation value of all formulas.

Modifier	Rutting parameter	Validation	
		k	k'
NHL	$(G^*/\sin\delta)_{NHL\%Unaged}$	0.986	0.982
	$(G^*/\sin\delta)_{NHL\%Aged}$	1.002	0.993
NC	$(G^*/\sin\delta)_{NC\%Unaged}$	1.006	0.997
	$(G^*/\sin\delta)_{NC\%Aged}$	0.991	0.990
NOH	$(G^*/\sin\delta)_{NOH\%Unaged}$	0.979	0.971
	$(G^*/\sin\delta)_{NOH\%Aged}$	0.986	0.981

3.5 Evaluation of model performance

Key statistical metrics were employed to quantify the accuracy and reliability of the GEP model and evaluate its predictive performance. These metrics provide indications of how well

the model aligns with experimental data. The R^2 , MAE, and RMSE were utilized for this analysis. Eqs. (11)-(13) define these statistical parameters.

$$R^2 = \frac{(\sum_{i=1}^N (X_i - \bar{X})(Y_i - \bar{Y}))^2}{\sum_{i=1}^N (X_i - \bar{X})^2 \sum_{i=1}^N (Y_i - \bar{Y})^2} \tag{11}$$

$$MAE = \frac{1}{N} \sum_{i=1}^N |X_i - Y_i| \tag{12}$$

$$RMSE = \sqrt{\frac{1}{N} \sum_{i=1}^N (X_i - Y_i)^2} \tag{13}$$

Table 8 presents the performance metrics of the prediction models for the rutting parameter ($G^*/\sin\delta$) for three modifiers: NHL, NC, and NOH, under unaged and aged conditions. The models demonstrate high predictive accuracy, as evidenced by consistently high R^2 values, frequently exceeding 0.97.

In the NHL, the unaged condition exhibits remarkable accuracy with $R^2 = 0.997$ (training) and $R^2 = 0.993$ (validation), along with minimal MAE and RMSE values. However, while R^2 remains strong at 0.966 in the aged condition, the higher error metrics (MAE = 0.471 and RMSE = 0.605 for training) suggest a more challenging prediction scenario. NC achieves the highest accuracy among the modifiers in the unaged state, with $R^2= 0.998$ for training and $R^2= 0.989$ for validation, accompanied by relatively low MAE and RMSE values. NC performs very well in the aged condition, with reduced validation errors (MAE = 0.314, RMSE = 0.384) compared to training, indicating excellent generalization capability. NOH demonstrates robust performance. While the unaged condition exhibits slightly lower accuracy ($R^2= 0.980$, for training and $R^2= 0.974$, for validation), the aged condition achieves outstanding results, with $R^2= 0.994$, for training and $R^2= 0.970$, for validation, coupled with minimal error values. Overall, these results confirm the reliability of the models, with each modifier demonstrating strong predictive performance across unaged and aged conditions.

4. Conclusion

This study evaluated the influence of nano-hydrated lime (NHL), nano-clay (NC), and nano-olive husk (NOH) on the

Table 8: GEP Statistical analysis for the training and validation value of all formulas.

Modifier	Rutting parameter	Training			Validation		
		R^2	MAE	RMSE	R^2	MAE	RMSE
NHL	$(G^*/\sin\delta)_{NHL\%Unaged}$	0.997	0.048	0.062	0.993	0.103	0.111
	$(G^*/\sin\delta)_{NHL\%Aged}$	0.966	0.471	0.605	0.966	0.549	0.680
NC	$(G^*/\sin\delta)_{NC\%Unaged}$	0.998	0.066	0.086	0.989	0.162	0.193
	$(G^*/\sin\delta)_{NC\%Aged}$	0.993	0.612	0.752	0.998	0.314	0.384
NOH	$(G^*/\sin\delta)_{NOH\%Unaged}$	0.980	0.087	0.116	0.974	0.103	0.136
	$(G^*/\sin\delta)_{NOH\%Aged}$	0.994	0.041	0.051	0.970	0.093	0.108

rutting performance of bitumen. This was achieved by assessing the parameter ($G^*/\sin\delta$) of unaged and short-term aged nanomodified bitumen. The dynamic shear rheometer (DSR) tests were conducted on bitumen samples modified with four concentrations of nanomaterials (1%, 3%, 5%, and 10% by bitumen weight). Consequently, predictive models were developed to estimate the $G^*/\sin\delta$ values of original and nanomodified bitumen. The results demonstrated that nanomodified bitumen exhibited significantly enhanced rutting resistance compared to original bitumen. Adding varied percentages of NHL enhanced the $G^*/\sin\delta$ value in unaged and short-term aged samples, with the most significant improvement being at 5% NHL; however, 10% NHL reduced the rutting parameter. It is postulated that the adverse effect of a 10% NHL concentration was caused by particle agglomeration. Performance of NHL-modified bitumen can be improved by ensuring uniform dispersion of nanoparticles. Adding NC increased the $G^*/\sin\delta$ value for unaged and short-term aged bitumen, with the highest being at 10% NC. Moreover, the incorporation of NOH by up to 5% increased the $G^*/\sin\delta$ value, after which the value decreased for both unaged and short-term aged samples. The presence of oil in NOH at concentrations of 10% and possible particle agglomeration seems to have affected its performance. The predictive GEP models' validity and robustness were confirmed through various statistical evaluation metrics and established benchmarks. For future research, it is recommended that different bitumen sources are incorporated in experiments that examine performance under various conditions (rutting, fatigue cracking, and low-temperature cracking). The effect of the type and content of oil in NOH on its performance as a bitumen modifier should also be studied further.

Acknowledgement

This work was fully funded by the Deanship of Scientific Research at Al-Ahliyya Amman University (Grant number 3/19/2023-2024).

Conflict of Interest

There is no conflict of interest.

Supporting Information

Not applicable.

References

- [1] Y. Tileuberdi, Y. Ongarbayev, Y. Imanbayev, A. Yermekova, F. Behrendt, A. Ismailova, K. Zhanbekov, A. Seilkhan, Z. Mansurov, Studying characteristics of natural bitumen of oil sand with comparison to heavy crude oil, *ES Materials & Manufacturing*, 2023, **22**, 1035 doi: 10.30919/esmm1035.
- [2] U. Kuoshiken, Y. Tileuberdi, Q. Shi, Y. Ongarbayev, S. Li, K. Zhanbekov, E. Kanzharkan, Y. Imanbayev, ESI FT-ICR MS analysis of polar compounds in natural bitumen of munaily-mola oil sands and its asphaltenes, *ES Materials & Manufacturing*, 2024, **25**, 1240, doi: 10.30919/esmm1240.
- [3] M. A. Franesqui, J. Yepes, C. García-González, J. Gallego, Sustainable low-temperature asphalt mixtures with marginal porous volcanic aggregates and crumb rubber modified bitumen, *Journal of Cleaner Production*, 2019, **207**, 44-56, doi: 10.1016/j.jclepro.2018.09.219.
- [4] S. N. Mahdi, T. Imjai, C. Wattanapanich, R. Garcia, H. Kaur, M. A. Musarat, Life cycle cost analysis of flexible pavements reinforced with geosynthetics: a case study of new construction or repair overlays in Thailand's roads, *Engineered Science*, 2024, **28**, 1071, doi: 10.30919/ES1071.
- [5] B. Teltayev, A. Massanov, Y. Aitbayev, A. Zhaisanbayev, Performance of a semi-rigid pavement: a north Kazakhstan case study, *Engineered Science*, 2024, **29**, 1089, doi: 10.30919/es1089.
- [6] A. H. Zghair Chfat, H. Yaacob, N. H. Mohd Kamaruddin, Z. H. Al-Saffar, R. Putra Jaya, Effects of nano eggshell powder as a sustainable bio-filler on the physical, rheological, and microstructure properties of bitumen, *Results in Engineering*, 2024, **22**, 102061, doi: 10.1016/j.rineng.2024.102061.
- [7] S. C. Dimri, R. Indu, M. Bajaj, R. S. Rathore, V. Blazek, A. K. Dutta, S. Alsubai, Modeling of traffic at a road crossing and optimization of waiting time of the vehicles, *Alexandria Engineering Journal*, 2024, **98**, 114-129, doi: 10.1016/j.aej.2024.04.050.
- [8] F. Qadir, I. Hafeez, Effect of impregnated organophilic (hydrophobic) nano clay on asphalt binder properties and performance, *Construction and Building Materials*, 2024, **419**, 135577, doi: 10.1016/j.conbuildmat.2024.135577.
- [9] S. H. Mousavinezhad, G. H. Shafabakhsh, O. Jafari Ani, Nano-clay and styrene-butadiene-styrene modified bitumen for improvement of rutting performance in asphalt mixtures containing steel slag aggregates, *Construction and Building Materials*, 2019, **226**, 793-801, doi: 10.1016/j.conbuildmat.2019.07.252.
- [10] S. A. Ghanoon, J. Tanzadeh, M. Mirsepahi, Laboratory evaluation of the composition of nano-clay, nano-lime and SBS modifiers on rutting resistance of asphalt binder, *Construction and Building Materials*, 2020, **238**, 117592, doi: 10.1016/j.conbuildmat.2019.117592.
- [11] A. Zahid, S. Ahmed, M. Irfan, Experimental investigation of nano materials applicability in hot mix asphalt (HMA), *Construction and Building Materials*, 2022, **350**, 128882, doi: 10.1016/j.conbuildmat.2022.128882.
- [12] R. M. Alfaqawi, A. Fareed, S. B. A. Zaidi, G. D. Airey, A. Rahim, Effect of hydrated lime and other mineral fillers on stiffening and oxidative ageing in bitumen mastic, *Construction and Building Materials*, 2022, **315**, 125789, doi: 10.1016/j.conbuildmat.2021.125789.
- [13] A. Rasouli, A. Kavussi, M. J. Qazizadeh, A. H. Taghikhani,

- Evaluating the effect of laboratory aging on fatigue behavior of asphalt mixtures containing hydrated lime, *Construction and Building Materials*, 2018, **164**, 655-662, doi: 10.1016/j.conbuildmat.2018.01.003.
- [14] A. S. Mohammed, A. Kavussi, M. Manteghian, The role of physical and chemical methods of nanohydrated lime production on properties of bituminous binders, *Construction and Building Materials*, 2024, **451**, 138794, doi: 10.1016/j.conbuildmat.2024.138794.
- [15] M. Arabani, M. Sadeghnejad, J. Haghanipour, M. H. Hassanjani, The influence of rice bran oil and nano-calcium oxide into bitumen as sustainable modifiers, *Case Studies in Construction Materials*, 2024, **21**, e03458, doi: 10.1016/j.cscm.2024.e03458.
- [16] A. N. S. Al Qadi, T. S. Khedaywi, M. A. Haddad, O. A. Al-Rababa'ah, Investigating the effect of olive husk ash on the properties of asphalt concrete mixture, *Annales de Chimie - Science Des Matériaux*, 2021, **45**, 11-15, doi: 10.18280/acsm.450102.
- [17] T. S. Khedaywi, M. A. Haddad, A. N. S. Al Qadi, O. A. Al-Rababa'ah, Investigating the effect of addition of olive husk ash on asphalt binder properties, *Annales de Chimie - Science Des Matériaux*, 2021, **45**, 239-243, doi: 10.18280/acsm.450307.
- [18] M. Haddad, T. Khedaywi, Investigating the effect of olive husk ash on dynamic creep of asphalt concrete mixtures, *Journal of Engineering Science and Technology*, 2024, **18**, 931-948.
- [19] T. Geckil, S. Issi, C. B. Ince, Evaluation of prina for use in asphalt modification, *Case Studies in Construction Materials*, 2022, **17**, e01623, doi: 10.1016/j.cscm.2022.e01623.
- [20] G. Aitkaliyeva, S. Azat, I. Baidullayev, R. Mangazbayeva, A. Amitova, M. Yelubay, G. Toleutay, A. Ismailova, I. Orazymbek, M. Abutalip, Using oil sludge as a rejuvenator for reclaimed asphalt pavement: improving sustainability in road maintenance, *ES Materials & Manufacturing*, 2024, **26**, 1291, doi: 10.30919/esmm1291.
- [21] D. N. Kontoni, K. C. Onyelowe, A. M. Ebid, H. Jahangir, D. Rezazadeh Eidgahee, A. Soleymani, C. Ikpa, Gene expression programming (GEP) modelling of sustainable building materials including mineral admixtures for novel solutions, *Mining*, 2022, **2**, 629-653, doi: 10.3390/mining2040034.
- [22] M. F. Javed, M. N. Amin, M. I. Shah, K. Khan, B. Iftikhar, F. Farooq, F. Aslam, R. Alyousef, H. Alabduljabbar, Applications of gene expression programming and regression techniques for estimating compressive strength of bagasse ash based concrete, *Crystals*, 2020, **10**, 737, doi: 10.3390/cryst10090737.
- [23] S. Matarneh, T. Alkhrrissat, M. Abdel-Jaber, The effect of pre-heating duration and temperature conditioning on rheological and rotational viscosity of asphalt bitumen modified with nano clay, nano hydrated lime, and nano olive husk binders, *Engineered Science*, 2025, **34**, 1376, doi: 10.30919/es1376.
- [24] ASTM D7175, ASTM D7175 test method for determining the rheological properties of asphalt binder using a dynamic shear rheometer, ASTM International, West Conshohocken, PA, 2023, doi: 10.1520/D7175-23.
- [25] Y. Erkuş, B. Vural Kök, Comparison of physical and rheological properties of calcium carbonate-polypropylene composite and SBS modified bitumen, *Construction and Building Materials*, 2023, **366**, 130196, doi: 10.1016/j.conbuildmat.2022.130196.
- [26] O. de Medeiros Melo Neto, A. A. Ferreira, T. de Souza Freire, G. C. B. da Silva, L. C. de Figueirêdo Lopes Lucena, V. F. de Sousa Neto, Rheological analysis of asphalt binders modified with hydrated lime and titanium dioxide nanoparticles, *International Journal for Innovation Education and Research*, 2020, **8**, 579-598, doi: 10.31686/ijer.vol8.iss11.2787.
- [27] A. D. Barros, L. C. de F. Lopes Lucena, D. B. Costa, Rheological properties of hydroxide and calcium oxide nanoparticles in asphalt binder, *Petroleum Science and Technology*, 2017, **35**, 738-745, doi: 10.1080/10916466.2016.1252774.
- [28] A. Diab, Z. P. You, H. N. Wang, Using modified creep and recovery tests to evaluate the foam-based warm mix asphalt contained nano hydrated lime, *Advanced Materials Research*, 2013, **646**, 90-96, doi: 10.4028/www.scientific.net/amr.646.90.
- [29] A. S. Mohammed, A. Kavussi, M. Manteghian, The role of nanomaterials in enhancing adhesion properties between bitumen and aggregate particles, *Results in Engineering*, 2024, **24**, 103193, doi: 10.1016/j.rineng.2024.103193.
- [30] A. Sadat Hosseini, P. Hajikarimi, M. Gandomi, F. Moghadas Nejad, A. H. Gandomi, Genetic programming to formulate viscoelastic behavior of modified asphalt binder, *Construction and Building Materials*, 2021, **286**, 122954, doi: 10.1016/j.conbuildmat.2021.122954.
- [31] H. Jia, S. Shi, D. Wu, H. Rao, J. Zhang, L. Abualigah, Improve coati optimization algorithm for solving constrained engineering optimization problems, *Journal of Computational Design and Engineering*, 2023, **10**, 2223-2250, doi: 10.1093/jcde/qwad095.
- [32] G. N. Smith, Probability and statistics in civil engineering, Collins Professional and Technical Books, Nichols Publishing Company, 1986.
- [33] A. Golbraikh, A. Tropsha, Beware of Q2!, *Journal of Molecular Graphics and Modelling*, 2002, **20**, 269-276, doi: 10.1016/s1093-3263(01)00123-1.

Publisher's Note: Engineered Science Publisher remains neutral with regard to jurisdictional claims in published maps and institutional affiliations.

Open Access

This article is licensed under a Creative Commons Attribution 4.0 International License, which permits the use, sharing, adaptation, distribution and reproduction in any medium or format, as long as appropriate credit to the original author(s) and the source is given by providing a link to the Creative Commons license and changes need to be indicated if there are any. The images or other third-party material in this article are included in the article's Creative Commons license, unless indicated otherwise in a credit line to the material. If material

is not included in the article's Creative Commons license and your intended use is not permitted by statutory regulation or exceeds the permitted use, you will need to obtain permission directly from the copyright holder. To view a copy of this license, visit <http://creativecommons.org/licenses/by/4.0/>.

©The Author(s) 2025